Surface & Coatings Technology 232 (2013) 419–424

Contents lists available at ScienceDirect

Surface & Coatings Technology

journal homepage: www.elsevier.com/locate/surfcoat

Nano–nano composite powders of lanthanum–gadolinium zirconate and gadolinia-stabilized zirconia prepared by spray pyrolysis

Songbai Liu [a,b], Kuo Jiang [b,*], Hongbo Zhang [c], Yi Liu [b], Li Zhang [b], Bingye Su [b], Yibao Liu [a]

[a] Department of Nuclear Engineering and Geophysics, East China Institute of Technology, Nanchang 330013, China
[b] Department of Defence Science and Technology, Southwest University of Science and Technology, Mianyang 621010, China
[c] Ceramics Science Institute, China Building Materials Academy, Beijing 100024, China

ARTICLE INFO

Article history:
Received 30 March 2013
Accepted in revised form 28 May 2013
Available online 5 June 2013

Keywords:
Nanocomposites
Lanthanum–gadolinium zirconate
Gadolinia-stabilized zirconia
Grain size
Spray pyrolysis
Doping behavior

ABSTRACT

Ceramics with structure on nanometer-length scales have a thermal conductivity much lower than their coarser-grained ceramics. But the relatively low activation energy for grain growth of nanoparticles limits the stability of nano-material at high temperatures. The objective of the present study was to investigate the preparation of the composite powders of nano $(La,Gd)_2Zr_2O_7$ and nano $(Zr,Gd)O_{2-\delta}$ by a sol-spray pyrolysis method. The XRD results indicated that the reaction products of $0.2LaO_{1.5}$–$xGdO_{1.5}$–$(0.8-x)ZrO_2$ $(0.15 \le x \le 0.25)$ ternary system were composed of pyrochlore $(La,Gd)_2Zr_2O_7$ and cubic $(Zr,Gd)O_2$ phases. The composition with $0.2LaO_{1.5}$–$0.2GdO_{1.5}$–$0.6ZrO_2$ had a grain size much smaller than the lower $GdO_{1.5}$ content counterpart for both the $(La,Gd)_2Zr_2O_7$ and $(Zr,Gd)O_{2-\delta}$ phases. The relationship between grain size and $GdO_{1.5}$ content was explained in terms of lattice matching.

1. Introduction

Ceramics with structure on nanometer-length scales have received steadily growing attention because of their peculiar and fascinating magnetic, electrical, optical, thermal and mechanical properties superior to their coarser-grained ceramics [1–4]. For example, the room temperature thermal conductivity of a 30 nm grain-sized yttria-stabilized zirconia (YSZ) was reported to be more than 50% lower than bulk YSZ [3]. However, the relatively low activation energy for grain growth of nanoparticles limits the stability of nano-material at the service temperatures higher than 1000 °C typically required of thermal barrier coatings (TBCs) [1].

As is well known, the addition of second phase particles causes grain boundary motion to drag [5,6]. This effect was considered as a powerful tool to control the microstructure and stability of grains [6]. Recently, the nanopowders of 8 mol% La_2O_3–8YSZ composite oxides were reported to have a smaller grain size than 8YSZ in the temperature range of 200–1300 °C [7]. This phenomenon can be attributed to grain boundary motion to drag from the $La_2Zr_2O_7$ particles of the composite powders.

$La_2Zr_2O_7$ with pyrochlore (P) structure is a promising candidate for the TBC of the future because of its phase stability, high melting point, and low thermal conductivity [8]. Lehmann et al. [9] systematically examined the influence of partial or complete substitution of La^{3+} by Nd^{3+}, Eu^{3+}, Gd^{3+}, and Dy^{3+} on the thermo-physical properties of $La_2Zr_2O_7$. Among these trivalent cations, Gd^{3+} ion was found to be one of the most effective rare-earth ions for lowering the thermal conductivity and improving the thermal expansion coefficient of $La_2Zr_2O_7$. In addition, both the thermal conductivity and sinter shrinkage of 4 mol% Gd_2O_3-stabilized ZrO_2 were reported to be lower than YSZ of the same composition [10].

Based on above research, it is expected that the composite powders composing of nanocrystalline $(La,Gd)_2Zr_2O_7$ and nanocrystalline $(Zr,Gd)O_{2-\delta}$ could be of an extreme low thermal conductivity. The objective of the present study was to investigate the phase composition and crystal structure of the reaction products of $LaO_{1.5}$–$GdO_{1.5}$–ZrO_2 ternary system from the in-situ reaction. The mechanism of controlling rare-earth oxide ($REO_{1.5}$) doping behavior in the $La_2Zr_2O_7$–ZrO_2 system was also studied via substitution of $GdO_{1.5}$ by $YO_{1.5}$ and $NdO_{1.5}$ in the ternary system.

2. Experimental

2.1. Powder synthesis

In the present study, 99.99% purity $Zr(NO_3)_4 \cdot 3H_2O$, $La(NO_3)_3 \cdot 6H_2O$ and $Gd(NO_3)_3 \cdot 6H_2O$ (Aladdin Chemistry Co. Ltd., Shanghai, China) were used as the starting materials and were dissolved in the deionized water. The total concentration of Zr^{4+}, La^{3+} and Gd^{3+} was 0.1 M, to which 80 g/L citric acid ($C_6H_8O_7 \cdot H_2O$) and 50 g/L polyethylene glycol (PEG, molecular weight = 20,000) were added to the starting solution. The solution was stirred with a magnetic stirrer for 30 min to achieve complete dissolution.

---

[*] Corresponding author. Tel.: +868162419010
E-mail address: jiangkuo@swust.edu.cn (K. Jiang).

0257-8972/$ – see front matter © 2013 Elsevier B.V. All rights reserved.
http://dx.doi.org/10.1016/j.surfcoat.2013.05.044

The resulting solution was then poured into a polytetrafluoroethylene (PTFE) tube and was atomized by using an atomizer. The atomizing device consisted of a sol supply, an atomizing medium gas supply, a stainless steel nozzle and a programmable high-temperature furnace, where 99.9% purity N_2 gas was used as the atomizing medium, and the pyrolysis temperature was 500 °C. The products were annealed at 900–1400 °C for 10–24 h in high-purity Al_2O_3 crucibles and were cooled down to room temperature in air.

2.2. Characterization

X-ray diffraction (XRD) analysis for the samples was carried out on an X' Pert PRO diffractometer with Cu Kα radiation ($\lambda = 0.15406$ nm; PANalytical, Almelo, Netherlands). The XRD patterns were collected in a 2θ range of 10°–90° at room temperature at a scanning rate of 0.05°/s and a step size of 0.033°. The peak positions and FWHM of the XRD peaks were determined using an X' Pert HighScore Plus software (version 2.0, PANalytical B. V., Almelo, Netherlands). The crystallite size was calculated using the Scherrer's formula for (440) and (220) peaks of pyrochlore and cubic zirconia phases, respectively: $D = 0.89\lambda / \beta\cos\theta$, where D is the crystallite size (in nm), λ is the wavelength (in nm), β is the FWHM, and θ is the diffraction angle.

Raman spectra of the samples were measured by a Renishaw InVia Raman spectrometer (Renishaw plc, New Mills, UK), with a spectrum resolution of 1 cm^{-1}. The excitation source of the emission line used was an Ar^+ ion laser of 514.5 nm.

The powders annealed at 900 °C were compacted in an 8 mm diameter steel die (applied pressure ≈ 500 MPa) to give pellets with a height of ~3 mm. The compacts were sintered at 1300 °C for 48 h in air (heating and cooling rates = 2 °C/min; SSX-8-16, Y-feng Electrical Furnace Co. Ltd., Shanghai, China). The samples of the bulk were observed using a field emission scanning electron microscopy (FE-SEM, Apollo 300 FE, Obducat CamScan Ltd., Cambridge, UK) operated at 30 kV.

The powders were ultrasonically dispersed in acetone and the resulting suspension was placed on a carbon-coated copper mesh grid. The TEM observation of the samples was obtained using a transmission electron microscope (TEM; JEM-2010, JEOL, Tokyo, Japan).

3. Results and discussion

3.1. Characteristics of prepared powders

The XRD patterns of $(La_{1-x}Gd_x)_2Zr_2O_7$ (x = 0–1.0) powders after annealing at 1200 °C for 24 h are shown in Fig. 1(a). The peaks at 2θ = 14.2°, 36.2° and 43.5° respectively correspond to the (111), (331) and (511) reflections of $La_2Zr_2O_7$, characteristic of pyrochlore structure. With increasing Gd content in $(La_{1-x}Gd_x)_2Zr_2O_7$ solid solution, the diffraction angle of the peaks of above patterns was altered, and the characteristic of pyrochlore structure vanished when x values were higher than 0.8. Fig. 1 (b) shows the XRD patterns and Raman spectra of $Gd_2Zr_2O_7$ sample after annealing at 1200 °C for 24 h and 1400 °C for 10 h. After a heat treatment of 1400 °C, the XRD peaks correspond to the (111), (311), (331) and (511) reflections of $Gd_2Zr_2O_7$ displayed, attributable to the pyrochlore structure. In the case of the Raman spectra, see the inset of Fig. 1 (b), the bands at 298, 392, 493, and 511 cm^{-1} were assigned to the Raman active vibration modes for the pyrochlore $La_2Zr_2O_7$ [11]. The corresponding bands for the $Gd_2Zr_2O_7$ annealed at 1400 °C were displayed at 317, 398, 538, and 602 cm^{-1}, and the bands mentioned above for the $Gd_2Zr_2O_7$ annealed at 1200 °C were obscure. The weakening of the XRD peaks, the broadening and merging of the Raman spectrum for the $Gd_2Zr_2O_7$ annealed at 1200 °C could be attributed to the defect-, furface-, size-related features of nanoparticles [12].

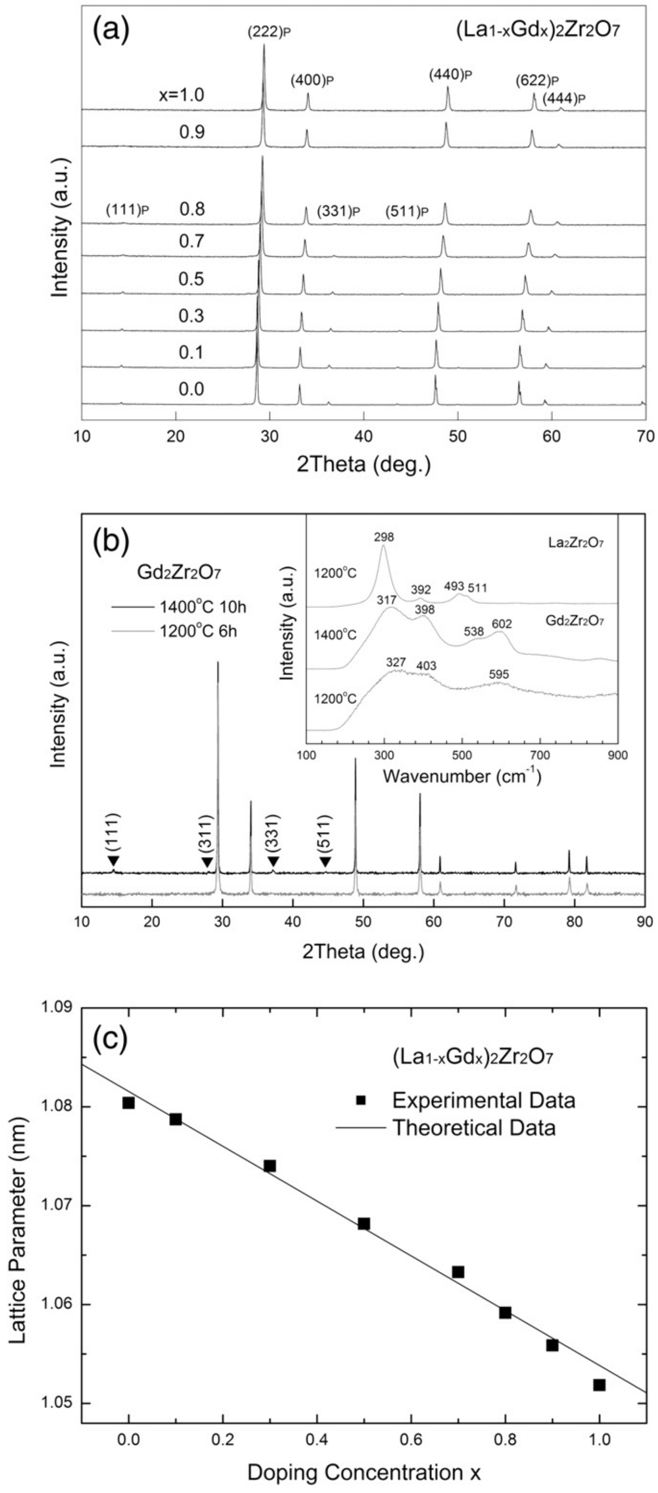

Fig. 1. (a) XRD patterns of $(La_{1-x}Gd_x)_2Zr_2O_7$ (x = 0–1.0) powders after annealing at 1200 °C for 24 h in air; (b) XRD patterns of $Gd_2Zr_2O_7$ sample after annealing at 1200 °C for 24 h and 1400 °C for 10 h in air (Inset: Raman spectra of $La_2Zr_2O_7$ and $Gd_2Zr_2O_7$ annealed at 1200 °C–1400 °C; and (c) Calculated lattice parameters from Bragg's law.

The lattice parameter (a) of the P-type phase can be calculated by using the following equation on the basis of Vegard's rule: [13–15]

$$\alpha = \left(8/\sqrt{3}\right)\left[0.5\, r\left(Ln^{3+}_{av.}\right) + 0.5\, \mathrm{r}\left(\mathrm{Zr}^{4+}\right) + 0.875\, \mathrm{r(O)} + 0.125\, \mathrm{r}(\mathrm{V_O})\right] \quad (1)$$